WPJET1-CPR(18) 19158

A Czarnecka et al.

Analysis of metalic impurity content by means of VUV and SXR diagnostics in the presence of ICRF induced hot-spot on the JET-ILW poloidal limiter

Preprint of Paper to be submitted for publication in Proceeding of 18th Topical Conference on High Temperature Plasma Diagnostics (HTPD)

This work has been carried out within the framework of the EUROfusion Consortium and has received funding from the Euratom research and training programme 2014-2018 under grant agreement No 633053. The views and opinions expressed herein do not necessarily reflect those of the European Commission.

Analysis of metallic impurity content by means of VUV and SXR diagnostics in the presence of ICRF induced hot-spot on the JET-ILW poloidal limiter [a)]

A. Czarnecka[1,b)], N. Krawczyk[1], P. Jacquet[2], E. Lerche[3], V. Bobkov[4], C. Challis[2], D. Frigione[5], J. Graves[6], K. D. Lawson[2], M.J. Mantsinen[7,8], L. Meneses[9], E. Pawelec[10], T. Pütterich[4], M. Sertoli[2], M. Valisa[11], D. Van Eester[3], and JET Contributors[c)]

EUROfusion Consortium, JET, Culham Science Centre, Abingdon, OX14 3DB, UK
[1]Institute of Plasma Physics and Laser Microfusion, Hery 23 Str., 01-497 Warsaw, Poland
[2]CCFE, Culham Science Centre, Abingdon, OX14 3DB, UK
[3]Laboratory for Plasma Physics, ERM/KMS, EUROfusion Consortium Member
Renaissancelaan 30, B-1000 Brussels, Belgium
[4]Max-Planck-Institut für Plasmaphysik, Boltzmannstr.2, D-85748, Germany
[5]ENEA, Fusion and Nuclear Safety Dep., C.R. Frascati, Frascati (Roma), Italy
[6]Ecole Polytechnique Fédérale de Lausanne (EPFL), Swiss Plasma Center (SPC), CH-1015 Lausanne, Switzerland
[7]ICREA, Barcelona, Spain
[8]Barcelona Supercomputing Center, Barcelona, Spain
[9]Associação EURATOM/IST, Instituto de Plasmas e Fusão Nuclear – Laboratório Associado, Instituto Superior Técnico, P-1049-001 Lisboa
[10]Institute of Physics, Opole University, Oleska 48 Str., 45-052 Opole, Poland

(Presented XXXXX; received XXXXX; accepted XXXXX; published online XXXXX)

This paper presents a methods for the intrinsic impurity concentration measurements by means of VUV and SXR diagnostics on the JET-ILW tokamak. Measurements of mid-Z impurities content were obtained by means of VUV spectra. To provide absolute concentrations a new relative calibration technique has been proposed. It's based on cross-calibration with a calibrated spectrometer by using the unresolved transition array of W in the relevant wavelength range. The SXR cameras were used to deduce W profiles and poloidal asymmetries. Focus is given to hybrid discharges stopped by the real-time vessel protection system due to hot-spots formation. This effect was linked to the application of ICRH power. Local D_2 gas injection allows mitigating hot-spot formation and run pulses with acceptable temperature values on vessel components. Hot-spot temperature analysis showed a lower maximum temperature at higher gas rate. A decrease of impurity concentration with D_2 injection rate was observed. Changes in the plasma current have a strong impact on the plasma-wall interaction, both via modifications in the edge density and in the fast-ion losses. Finally it was observed that at constant gas injection rate, both the hot-spots temperature and the core impurity content decrease with the separatrix density.

I. INTRODUCTION

Experimental campaigns performed at the tokamak JET in 2015-2016 were devoted to the optimisation of ITER regimes of operation in the presence of the ITER-Like Wall (ILW) and to the optimal preparation of the deuterium-tritium (DT) campaign. The development of operational scenarios is underway with the target to provide about 15 MW of maximum fusion power in the forthcoming JET DT experiment, maintaining steady high performance phase for ~5 seconds. This requires i) high power heating, ii) low neutral density (i.e. low gas injection rate and good pumping for weak power degradation of confinement), iii) balance between high plasma current (for high global confinement), and iv) low plasma density (for central beam deposition and high core temperature, $T_i > T_e$). The main challenge to achieve such conditions is high Z impurity accumulation, high divertor heat loads and MHD instabilities, since this is commonly the first performance degrading factor in hybrid plasmas. Good progress was made in both baseline and hybrid scenario and a new ILW fusion record of 2.9×10^{16} neutrons/s was achieved[1]. High-Z impurity control in the core of D-T scenarios with the Ion Cyclotron Resonance Heating (ICRH) was crucial for extending the duration of the high-performance phase[1]. For core impurity control, fundamental H minority heating as central as possible with low minority concentration has shown the best results so far in a large H-mode dataset[2-5], but dominant N=2 D heating as well as combined H+He^3 ICRH heating also proved to be effective in the few cases studied[6]. The main effects of ICRH that cause reduced impurity peaking are related to temperature peaking, density flattening and fast ion effects[7],

[a)] Published as part of the Proceedings of the 22nd Topical Conference on High-Temperature Plasma Diagnostics (HTPD 2018) in San Diego, California, USA.
[b)] Author to whom correspondence should be addressed: agata.czarnecka@ifpilm.pl
[c)] See the author list of "X. Litaudon et al 2017 Nucl. Fusion 57 102001″

so that the latter embeds both the anisotropy and the collisional processes. In this paper special focus is given to high-power hybrid discharges that were stopped by the real-time vessel protection system due to the formation of hot-spots on the poloidal limiter. This effect was linked to the application of high ICRH power ($P_{ICRH} \geq 5$ MW, dipole phasing, N=1 H minority ~2 %) on the top of high NBI power (P_{NBI} ~ 25 MW) in hybrid plasmas with magnetic field B_o=2.76 T, and plasma current I_p=2.2 MA (some with I_p=2.4 MA and 2.0 MA). FIG 1 is showing the image from a visible protection camera with the indicated high temperature region on the narrow poloidal limiter NPL3B close to the ICRH antenna B. It turned out that local deuterium (D_2) gas injection from the mid-plane Gas Injection Module (GIM6) allows mitigating hot-spot formation. The previously obtained experimental results showed that distributed mid-plane gas injection is the best

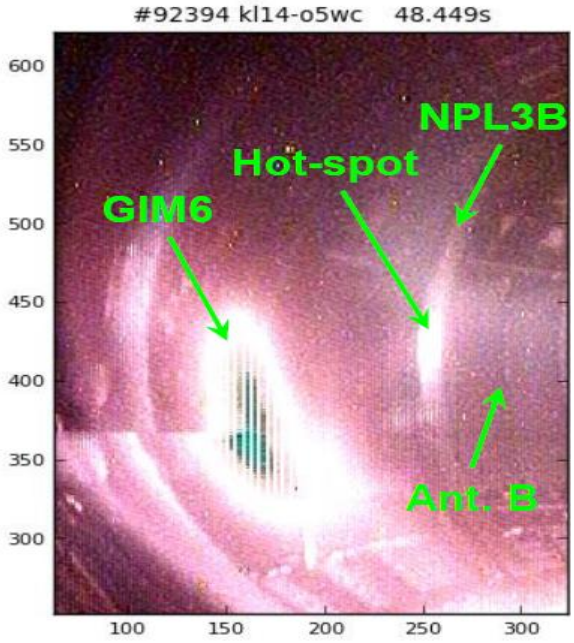

FIG. 1. Image form protection camera with the high temperature regions in the poloidal limiter NPL3B.

recipe for overall RF coupling improvement at gas levels compatible with high performance scenario development[3]. There are clear indications that this type of distributed gas injection also has a beneficial impact on RF-induced impurity content but the physics mechanisms behind such observation are still under study. Therefore, influence of D_2 gas injection on hot-spot temperature and high-, and mid-Z impurity measurements made by means of vacuum-ultra-violet (VUV) and soft X-ray (SXR) diagnostics at JET is presented in this paper.

II. DIAGNOSTICS AND ANALYSIS METHODS

A. VUV spectroscopy diagnostic

The VUV spectrometer known on JET as the KT2[8] diagnostic is routinely used to give impurity data for the operation of the JET machine. The diagnostic consists of the Princeton Instruments survey SPRED[9] (Survey, Poor Resolution, Extended Domain) spectrometer. The diagnostic has a horizontal line-of-sight (l-o-s) (illustrated in FIG. 2 as a red line) looking at the vessel mid-plane via an Au coating spherical mirror, allowing it to view the emission from the core and scrape-off layer of the plasma.

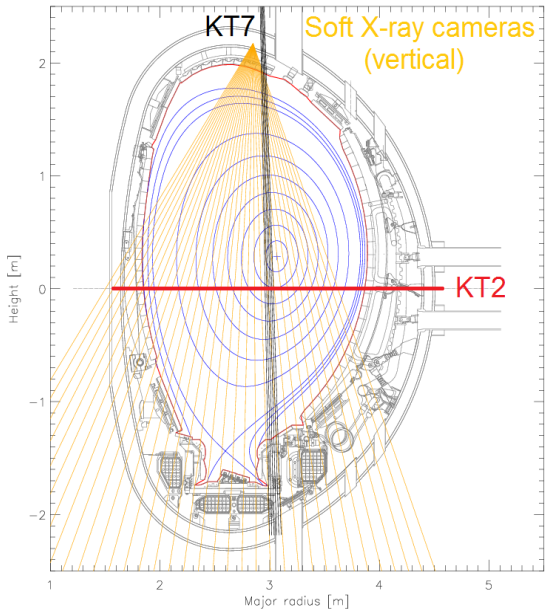

FIG. 2. Lines of sight of KT2 diagnostic (red horizontal line), KT7 diagnostic (black vertical line) and SXR vertical cameras (orange lines) at JET tokamak.

Signal is detected by a micro-channel plate (MCP) and a phosphor screen from which radiation is coupled by a fiber optic cable to a 2048 Photo Diode Array (PDA). The diagnostic is equipped with a 450 g/mm holographic grating and measures spectra in the 100–1100 Å wavelength range, with a spectral resolution of ~ 5 Å. The highest time resolution is 11 ms, although 50 ms is routinely used. With the carbon plasma facing components (PFC), the long wavelength of VUV spectrum was dominated by low-Z impurities like carbon (C) and oxygen (O), while the short wavelength range by different mid-Z impurities like nickel (Ni), iron (Fe), copper (Cu), chromium (Cr), molybdenum (Mo) making this range particularly valuable from the point of view of diagnosing high temperature plasmas. After installation of the ITER-like wall (ILW) at JET, which consists of a full tungsten (W) divertor and beryllium (Be) main chamber PFCs, the spectrum also contains intense W features (see FIG. 3 which shows recorded spectrum in TET Pulse No. (JPN) 92394). Be lines are only observed in the spectrum during limiter phase of the discharge.

1. New relative calibration method

In order to fully exploit the line intensity measurements, sensitivity calibration of the spectrometer is necessary. In the case of visible instruments both relative and absolute sensitivity calibrations can be determined using a standard calibration lamp. However, the use of a local calibration source for VUV spectrometers is experimentally very difficult and the removal of vacuum instruments from the

machine site to, for example, a synchrotron source is not possible due to beryllium contamination. As shown by Lawson et al.[10] it is possible to derive absolute sensitivity calibrations using the branching ratio between the C IV 312.4 Å VUV line and the lines at 5801 Å and 5812 Å from a calibrated visible spectrum and use in situ method which involve the use of Na- and Li-like line intensity ratios of different elements to obtain a relative sensitivity curve. The

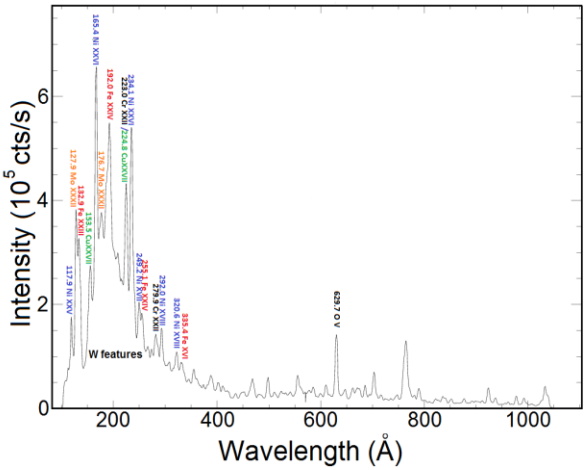

FIG. 3. SPRED spectrum for JET pulse No 92394 t=8-8.5 s

reduction of the C level in the JET-ILW plasmas impacted on the difficulties with the branching ratio technique, because C lines were only occasionally observed, mostly in transient events such as a disruption. Relative intensities are temperature-dependent, which adds the uncertainty to the relative calibrations. This method is also suitable only when lines are well separated, which means that spectrometers with higher spectral resolution are more easily calibrated. Therefore, to provide absolute mid-Z impurity concentrations a new relative calibration technique is proposed. It is based on cross-calibration with calibrated spectrometer using (simultaneous recordings of) the unresolved transition array (UTA) of W in the relevant wavelength range. Analysis of W ablation experiment shows that around 100 ms after ablation, in sufficiently cold plasma (with maximum temperature not exceeding 2 keV), the same radiating cloud of W is viewed by all the VUV spectrometers with different l-o-s (e.g. horizontal and vertical l-o-s of KT2 and KT7 diagnostic, respectively, presented in FIG. 2). This radiation provides a possible tool for cross-calibration of the relative inverse sensitivity of different VUV spectrometers, in the spectral regions where the W radiation is sufficiently strong. This is especially useful for the KT2 diagnostic with low spectral resolution and possible line blending (like Ni, Cu lines). The divertor-viewing VUV spectrometer, known locally as KT7/2 diagnostic on JET has higher resolution detector and an independent relative sensitivity calibration[11] which is unchanged since last calibration. In the case of to high core temperature, registered W spectra were too weak to have a proper signal to noise ratio and originated from relatively thin layer of plasma, which may not be symmetric and therefore different for horizontal and vertical l-o-s. As the radiation before and sufficiently after ablation was very similar, the difference of the spectra in studied temporal frames and the frames before ablation were considered as the "pure" ablated W spectrum. Thus the averaged spectra from 100 to 200 ms before and after ablation were subtracted to obtain the pure W spectrum. Curve of inverse sensitivity of KT2 diagnostic was calculated from the ratio of KT2 to KT7/2 spectrum multiplied by inverse sensitivity of KT7/2 diagnostic. Resulting curves obtained for different discharges are presented in FIG. 4. Tungsten spectra with the new calibration allowed to obtain the same shape of W spectrum from both diagnostics. The calibration results are showing large loss of detector sensitivity in the short-wavelength region in comparison to calibration made for C-wall[10]. It can be also seen, that the shapes of the relative calibration curves are pretty similar for different JET-ILW

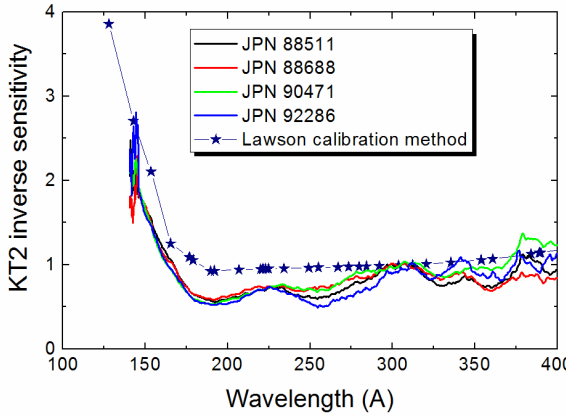

FIG. 4. Normalized average inverse sensitivities of KT2 diagnostic for four pulses with tungsten ablation experiments. Results are compared with calibration curves using K. Lawson's method.

campaigns, as the pulse numbers cover from 88500 to 92300. Resulting calibration is similar to the calibration curve obtained using method developed by Lawson et al.

The loss of sensitivity at short wavelengths is thought to be due to a deterioration in the grating coating. Less likely explanations are degradation of the CuI coating on the front face of the microchannel plate (MCP) or an absorbing deposited film within the channels themselves. It is noted that throughout the period in which a loss of sensitivity has been observed, the second order spectrum, which is normally absent from SPRED spectra, increased in intensity. This can only be explained by a change in the grating properties, providing further evidence of a change in the grating itself. The 165.4 Å, 192.0 Å and 153.5 Å spectral lines are used to determine respectively Ni, Fe and Cu concentrations in the plasma, using the method described in detail by Czarnecka et al. in Ref.[12]. This technique relies on the absolutely calibrated line intensities measured by the KT2 diagnostics, as well as simulations involving universal transport code (UTC)[13]. The electron density and temperature profiles from high resolution Thomson Scattering (HRTS) diagnostic are taken into account.

B. SXR diagnostic

The SXR diagnostic is used to quantify the amount of high-Z impurities in the main plasma of JET. The large number

of the vertical SXR cameras with different l-o-s (presented in FIG.2) allows determining the profiles of W-concentration and a 2D-profiles of SXR-radiation. In order to simulate the resulting signal of the vertical cameras, the 250 microns beryllium filter is taken into account. The l-o-s integrals are performed using their geometry and a magnetic equilibrium reconstruction from EFIT. Quantitative diagnosis of the W content in this approach is described in detail in Ref.[14]. To predict the local SXR emissivity due to Bremsstrahlung it is assumed that only Be, as the low-Z impurities, gives rise to Bremsstrahlung, while the only other radiator is W. This is implemented using the visible Bremmstrahlung Z_{eff} measurements. Contributions from mid-Z impurity is assumed negligible. However, it is not unambiguous what species in the plasma are responsible for the radiation in the soft X-ray range. Therefore, contribution of mid-Z impurities to Z_{eff} is examined in the paper using the VUV spectroscopic calculations.

III. RESULTS AND DISCUSSION

Hot spot temperature analysis presented in FIG. 5, performed using signals from the protection camera, showed the maximum temperature (T_{max}=940 °C) at lower gas rate. Dedicated investigations showed that local D_2 gas injection allows mitigating hot-spot formation, allowing the pulses to run with acceptable temperature values on protruding vessel components. As it is presented in FIG. 6, a decrease of the high- and mid-Z impurity concentration with D_2 gas injection rate was equally observed. The presented error bars are obtained by propagating an

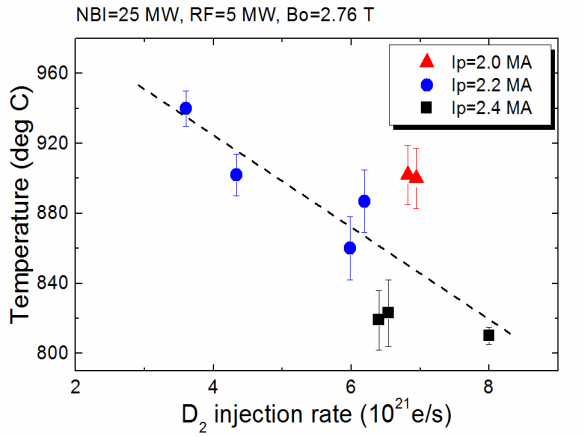

FIG. 5. Hot-spot temperature (averaged 0.5 s ~t=8 s) on the narrow poloidal limiter NPL3B determined form the protection camera signals as a function of D_2 gas injection rate from GIM6.

uncertainty of the measured line intensity, electron densities and temperatures. The same trend was observed in the behaviour of the Z_{eff} determined form visible spectroscopy diagnostic. Calculations of contribution mid-Z impurities to Z_{eff} (ΔZ_{eff}), by the use of data from VUV spectroscopy and the method described in Ref.[12], are presented in FIG. 7. It was found that highest ΔZ_{eff} comes from Ni. Different trend of hot spot temperature, impurity concentration and Z_{eff} is observed when plasma current (I_p) was changed. Changes in the I_p have a strong impact on the plasma-wall interaction,

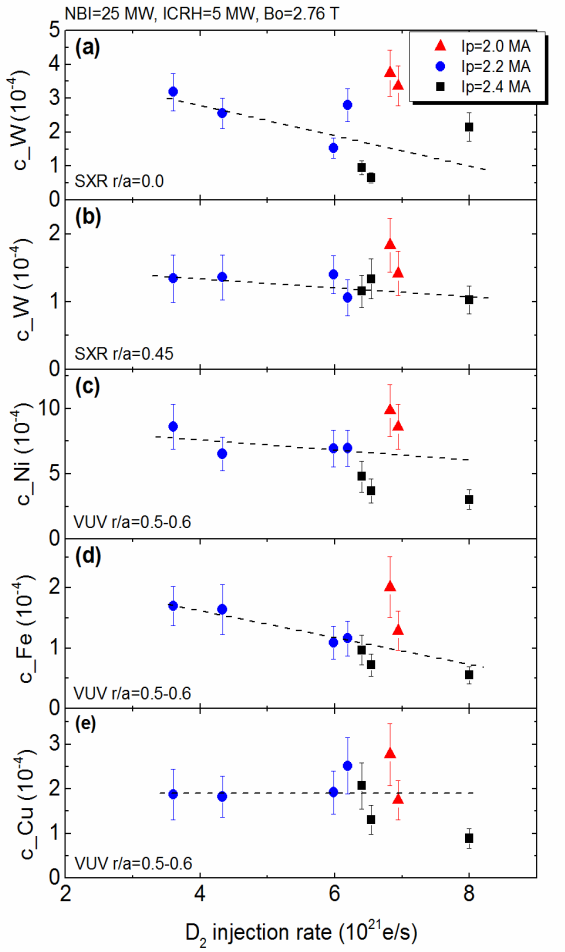

FIG. 6. Concentration of a) W at r/a=0.0, b) W at r/a=0.45 derived from SXR diagnostic and c) Ni at r/a=0.5-0.6, d) Fe at r/a=0.5-0.6, e) Cu at r/a=0.5-0.6 derived from VUV diagnostic as a function of D_2 injection rate for different plasma current Ip (averaged 0.5 s ~t=8 s).

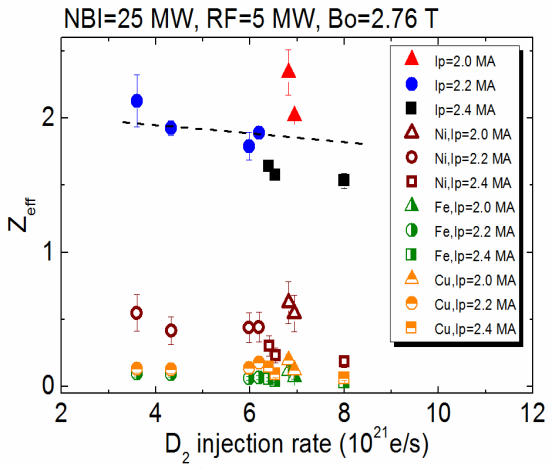

FIG. 7. Z_{eff} determined form visible spectroscopy diagnostic and contribution of Ni and Fe to Z_{eff} determined based on data from VUV spectroscopy diagnostic as a function of D_2 injection rate for different I_p (averaged 0.5 s ~t=8 s).

both via modifications in the edge density and in the fast-ion losses. FIG. 8 is showing metallic impurities concentrations in plasmas with different I_p at the same D_2

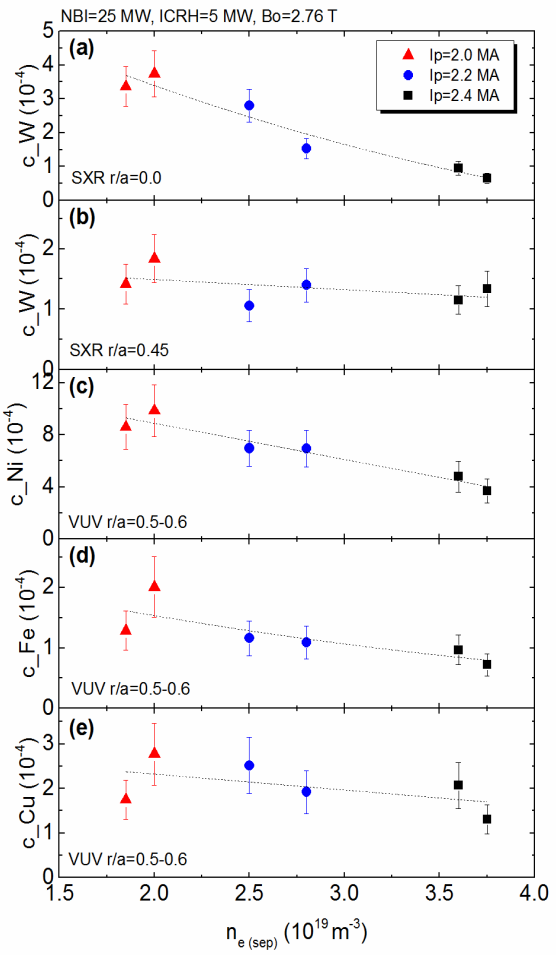

FIG. 8. Concentration of a) W at r/a=0.0, b) W at r/a=0.45 derived from SXR diagnostic and c) Ni at r/a=0.5-0.6, d) Fe at r/a=0.5-0.6, e) Cu at r/a=0.5-0.6 derived from VUV diagnostic as a function of separatrix density for different plasma current I_p (averaged 0.5 s ~t=8 s).

gas injection rate (~6×10^{21} e/s) as a function of separatrix density ($n_{e\ (sep)}$). It was observed that at constant gas injection rate, both the core metallic impurity content and the hot-spot temperature (not presented here) decrease with

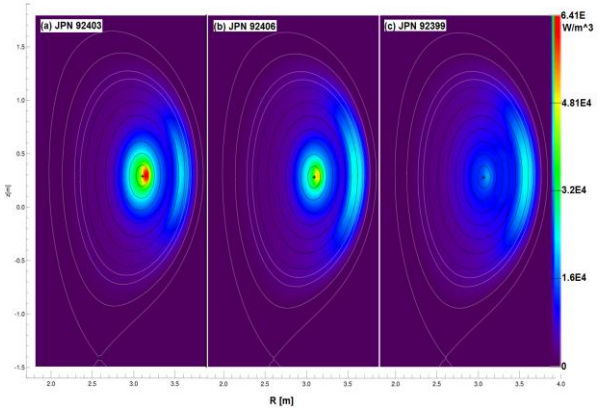

FIG. 9. 2D-profiles of SXR-radiation distributed over the JET poloidal cross-section for a) JPN 92403 with I_p = 2 MA, $n_{e\ (sep)}=2\times10^{19}$ m^{-3}, b) JPN 92406 with I_p = 2.2 MA, $n_{e\ (sep)}=2.5\times10^{19}$ m^{-3}, and c) JPN 92399 with I_p = 2.4 MA, $n_{e\ (sep)}=3.75\times10^{19}$ m^{-3}.

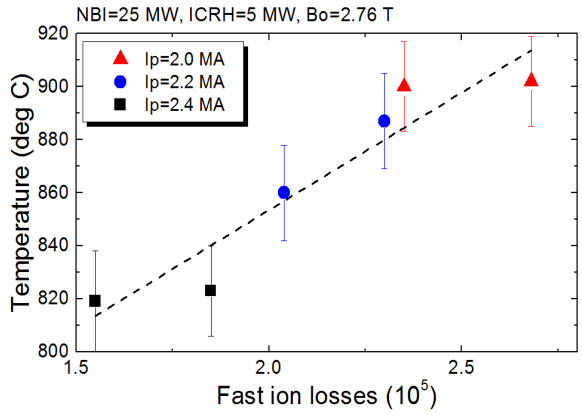

FIG. 10. Hot spot temperature (averaged 0.5 s ~t=8 s) on the narrow poloidal limiter NPL3B determined form the protection camera signals as a function of fast ion losses.

the $n_{e\ (sep)}$. In FIG. 9 occurred poloidal asymmetries can be easily observed and higher SXR radiation for lower $n_{e\ (sep)}$. As it can be seen in FIG.10 hot-spot temperature increase with fast-ion loses at constant gas rate.

IV. CONCLUSIONS

In some high power hybrid plasmas, strong ICRH-induced plasma wall interaction was observed to be caused by fast particle losses. This was verified by the correlation between the fast particle diagnostics measurements and the heat loads measured in specific outer wall Be limiters. The heat-loads could be efficiently minimized by local gas injection without affecting the core plasma properties. The changes in gas affect both hot-spots and impurity behaviour separately. Reduction of metallic impurities with D_2 gas injection rate was observed. One possible explanations is that the fast particle beam that hits a specific region of the limiter is somewhat diffracted by the higher SOL density and neutral pressure but a numerical assessment that would confirm such a theory is still ongoing.

V. ACKNOWLEDGMENTS

This work has been carried out within the framework of the EUROfusion Consortium and has received funding from the Euratom research and training programme 2014-2018 under grant agreement No 633053. The views and opinions expressed herein do not necessarily reflect those of the European Commission. This scientific work was partly supported by Polish Ministry of Science and Higher Education within the framework of the scientific financial resources in the year 2018 allocated for the realization of the international co-financed project.

VI. REFERENCES

[1]M. J. Mantsinen et al., European Physical Journal Web of Conferences **157**, 3032 (2017).

[2]M. Goniche et al., Plasma Physics and Controlled Fusion **59**, 055001 (2017).

[3]E. Lerche et al., Nuclear Fusion **56**, 036022 (2016).

[4]C. Angioni et al., Nuclear Fusion **54**, 083028 (2014).

[5]F. Casson et al., Plasma Physics and Controlled Fusion **57**, 014031 (2015).

[6]D. Van Eester et al., Proc. 26rd IAEA Fusion Energy, Kyoto, Japan, 17-22 October 2016, IAEA-CN-234, EX/P6-10.
[7]F. J. Casson et al., 19th Joint EU-US Transport Task Force Meeting, Culham, UK, 8-11 September 2014. https://users.euro-fusion.org/repository/pinboard/EFDA-JET/conference/archived/36334_casson_ttf_2014_4.pdf
[8]I. H. Coffey, R. Barnsley Rev Sci Instrum **75**, 3737 (2004).
[9]R. J. Fonck, A. T. Ramsey, R. V. Yelle Appl Optics **21**, 2115 (1982).
[10]K. D. Lawson, I. H. Coffey, J. Zacks, M. F. Stamp, J. Instrum. **4,** P04013 (2009).
[11]K. D. Lawson, K. M. Aggarwal, I. H. Coffey, F. P. Keenan, M. G. O'Mullane, L. Ryć, J. Zacks, Plasma Phys. Control. Fusion **53,** 015002 (2011).
[12]A. Czarnecka, K-D Zastrow, J. Rzadkiewicz, I. H. Coffey, K. D. Lawson, M. G. O'Mullane, Plasma Phys. Control. Fusion **53**, 035009 (2011).
[13]A. D. Whiteford *et al*., Proc. 31st EPS Conf., London, UK 28th June - 2nd July 2004, vol. 28G (ECA) P–1.159.
[14] T. Putterich et al., Proc. 24rd IAEA Fusion Energy Conf., San Diego, CA 8-13 October 2012 (Vienna: IAEA) vol. IAEA-CN-197, EX–P3.15.